J. Fluid Mech. (1980), *vol.* 97, *part* 2, *pp.* 321–330
Printed in Great Britain

Flow development of a highly viscous fluid emerging from a slit onto a plate

By A. STÜCHELI†

Institut für Verfahrenstechnik, Swiss Federal Institute of Technology, Zurich, Switzerland

(Received 17 August 1978 and in revised form 14 May 1979)

This paper is concerned with understanding the development of a free surface and the velocity of a thick creeping film emerging from a slit onto a plate. There is a difference between free surface flows with film thickness of 10 to 20 mm and thin film flows of less than 1 to 2 mm due to surface tension influence.

A laser–Doppler velocimeter of high spatial and temporal resolution has been used to measure the decreasing thickness of slowly flowing liquid and the velocity profiles at the exit of the slit and in the transition region of the plate. The hydrodynamic entrance length can be calculated from an empirical dimensionless relation that includes only the plate inclination angle β as a parameter.

1. Introduction

The purpose of this paper is to present highly accurate measurements of the transition of a gravitation-driven flow with parabolic velocity profile to a flow with semi-parabolic velocity distribution, i.e. the slit-to-plate flow, and to demonstrate the relative importance of each term of the Navier–Stokes equation. The experimental investigation was motivated by the question about the hydrodynamic entrance length that arose when heat transfer measurements on highly viscous falling liquid films were carried out (Stücheli 1978). If the Reynolds number $Re = Q\rho/\mu \gtrsim 100$ there exist theoretical and experimental investigations of Cerro & Whitaker (1971), Whitaker & Cerro (1974) as well as an analytical approximate solution of Stücheli & Özisik (1976). In this work Q is the volumetric discharge per plate width, ρ and μ are the density and the viscosity, respectively. Wilkes & Nedderman (1962) reported measurements of velocities in thin films of liquid obtained by the stereoscopic photography of small air bubbles moving with the fluid. However, the experiments were carried out in vertical position only with final film thickness h_∞ of 0·9 to 1·2 mm. They gave too little attention to the superimposed $\partial p/\partial x$ influence, i.e. external pressure in the slit of height h_0, as well as to the pressure induced by surface tension σ for h_0/h_∞ can never be smaller than $4\frac{1}{3}$ if $\sigma = 0$. It has to be the surface tension that made $h_0/h_\infty = 1{\cdot}8$ in their shown velocity profiles.

The problem for $Re \approx 1$ is still unsolved and no velocity profiles have been reported until today. Ruschak & Scriven (1977) analysed the developing laminar flow for the limiting case of very low flow-rate and high surface tension, respectively. In the first

† Present address: Research Division 1536, Sulzer Brothers Ltd. 8400 Winterthur, Switzerland.

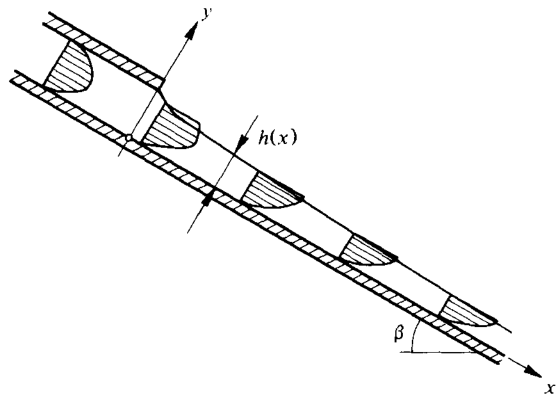

FIGURE 1. Flow situations in the slit and plate region.

case, the limiting profile of the free surface is an elastica determined entirely by a hydrostatic pressure field and the surface tension. In the second case of very large surface tension, the curvature of the free surface becomes uniformly small and the flow downstream of the slit is reflected in the nearly rectilinear nature.

Goren (1966) considers the development of the boundary layer at a free surface from a uniform shear flow. He omits gravitational force as well as surface tension. Owing to the absence of both a characteristic length and a characteristic velocity, this problem admits a similarity solution. The analysis shows that the surface velocity and the surface position vary as the cube root of the distance downstream.

2. The momentum equation

The hydrodynamic entrance flow problem of a Newtonian creeping falling liquid film (see figure 1) is completely determined by (Stücheli 1976):

(i) the momentum equation

$$3(\cot\beta - 1)\frac{dH}{dX} - \frac{Re}{We}\frac{d^2H/dX^2}{[1+(dH/dX)^2]^{\frac{3}{2}}} = \frac{\partial^2 U_s}{\partial X^2} + 2\frac{\partial^2 U}{\partial X^2} + \frac{\partial^2 U}{\partial Y^2}; \tag{1}$$

(ii) the constant flow condition

$$\int_0^{H(X)} U\,dY = 1; \tag{2}$$

(iii) the velocities and shear stresses, respectively,

$$U = \tfrac{3}{2}(4^{\frac{1}{3}}Y - Y^2) \quad \text{at} \quad X = 0, \tag{3}$$

$$U = \tfrac{3}{2}(2Y - Y^2) \quad \text{at} \quad X \to \infty, \tag{4}$$

$$U(X, 0) = 0 \quad \text{at} \quad Y = 0 \quad \text{(no slip at the wall)}, \tag{5}$$

$$\frac{\partial U}{\partial Y} - 3\frac{\partial U}{\partial X}\frac{dH}{dX} + 2U\frac{d^2H}{dX^2} = 0 \quad \text{at} \quad Y = H(X) \quad \text{(shear stress-free surface)}; \tag{6}$$

(iv) the surface shape conditions

$$H_0 = 4^{\frac{1}{3}} \quad \text{at} \quad X = 0, \tag{7}$$

$$\frac{dH}{dX} = 0 \quad \text{and} \quad \frac{d^2H}{dX^2} = 0 \quad \text{at} \quad X \to \infty. \tag{8), (9}$$

Property	Value	Source
Density ρ	889 kg/m^3 at 20 °C	Data sheet BASF
Volume expansion coefficient	6·7 10^{-4} K^{-1}	Data sheet BASF
Surface tension σ	31·4 10^{-3} N/m at 20 °C	LeGrand & Gaines (1969)
$\partial\sigma/\partial T$	$-6{\cdot}5\times 10^5$ Nm^{-1}K^{-1}	LeGrand & Gaines (1969)
Viscosity μ	302 P at 20·0 °C	Measurements evaluated from $h_\infty = (3Q\mu/\rho g \sin\beta)^{\frac{1}{3}}$
$\partial(\ln\mu)/\partial(1/T)$	6388	Calculated from own measurements

TABLE 1. Properties of polyisobutylene (BASF, OPPANOL B3).

The dimensionless quantities are all related to the developed-film flow quantities $\langle u\rangle_\infty$ and h_∞, We denotes the Weber number, which is defined as $Q\rho/\sigma h_\infty^2$. The numerical factor $4^{\frac{1}{3}}$ arises from the ratio $H_0 = h_0/h_\infty$ for gravitational driven slit flows, i.e. with no pressure gradient within the slit; otherwise a new parameter Fr/Re, including the Froude number, has to be considered. Equation (1) results from the combination of the equations of continuity, X momentum and Y momentum where only $\partial V/\partial X$ is disregarded by relative order-of-magnitude arguments.

3. Experimental system

3.1. *Flow apparatus and testing fluid*

A flow plane of 246 mm width was designed so it could be continuously inclined to within $\pm 5'$ over the range of β from 0° to 80°. It consisted of a constant-head device, a plexiglass slit and a falling-film plate also made to serve as the heating section for heat transfer measurements. The slit was 410 mm long and its height h_0 was adjustable to within $\pm 0{\cdot}02$ mm. The plate length was 390 mm. A change of the experimental parameter Re, the Reynolds number, could be achieved not only by different slit heights but also by alterations of the temperature of the testing fluid since this was preheated in a reservoir. The viscosity of the undiluted polyisobutylene (BASF, OPPANOL B3) is very temperature sensitive as shown in table 1. It is also worth noting that OPPANOL B3 behaves in a Newtonian manner because no shear-rate dependence of the viscosity and no normal stress effects (i.e., die swell) occurred in the experiments.

3.2. *The laser–Doppler velocimeter system*

A special He–Ne LDV system in the backscattering mode was used to get high spatial and temporal resolution. For the following system parameters – beam waist at the laser exit $2w_0 = 0{\cdot}65$ mm, distance $z_0 = 400$ mm between beam waist and focusing lens with focal length $f = 49{\cdot}29$ mm, beam separation $d = 30{\cdot}0$ mm and index of refraction of the liquid $n = 1{\cdot}487$ – the optical measuring volume has a length of $\Delta y = 183\,\mu$m and a diameter $\Delta d = 35\,\mu$m. The spatial uncertainty of the origin of the scattered signal or the spatial resolution, i.e. the ratio of Δy to the film thickness h, was further improved by forming with a telescope an image of the measuring volume four times larger, onto a tiny pinhole. Because the diameter of the pinhole was 50 μm, the electro-optical active length of the measuring volume decreased from 183 to 65 μm; the fringe distance was 1·087 μm. To get an excellent signal-to-noise ratio down to 100 Hz, i.e. 0·1 mm s^{-1} flow velocity, and a high temporal resolution, a fast-level discriminator and a logic-circuitry comparator were built as a real-time counter (see Iten & Mastner 1974).

Any movement of the optical system relative to the flow plane (due to small vibrations in a building) gives rise to incorrect amounts of the Doppler frequency. Therefore the experimental arrangement had to be rigidly connected. This vibration-induced frequency effect causes feigned velocity fluctuations and can never be neglected in very precise and low-velocity measurements. For that reason frequency shift devices such as Bragg cells cannot give more accurate results, they only ease the electronical signal processing.

3.3. *Measurement of the film thickness and shape*

By using the surface of the liquid film as a reflector, the tiny measuring volume acts as an optical touching device. Because the LDV system worked in the backscattering mode, one could observe the focusing with an ocular ($\times$ 30). Therefore, the accuracy of all film thickness measurements was $\pm$ 0·01 mm, that is the repeatability of positioning of the co-ordinate table (with the rigidly and vibrational-free mounted optics) allowing to traverse the flow plane.

4. Experimental results and discussion

4.1. *The slit exit flow*

By considering the flow situation on the upper plate near the slit exit (see figure 1), it turns out that the velocity changes enormously due to the sudden leaving the wall boundary. Hence the question arises: how far upstream will the velocity profile be influenced?

Figure 2 shows that we still get the fully parabolic velocity profile one slit height from the exit edge, at $X = x/h_0 = -1$. At $X = -0{\cdot}25$ the deviation from the fully-developed slit profile is still very weak. Measurements at $X = -0{\cdot}07$, corresponding to $x = -1{\cdot}25$ mm, could be carried out only by a rotation of the LDV beam system so that no optical distortion occurred. The velocity profiles shown in figure 2 are the same for measurements with different angles β from 20° to 80°, and for different slit heights, $h_0 = 12$, 15 and 18 mm. Schowalter & Allen (1975) had found in their investigations on tube exist (with $\partial p/\partial x > 0$) that the retroactive length is about twice the tube diameter.

4.2. *The plate inlet flow*

From figure 3 one can see a strong velocity rearrangement in the upper fluid region and that the surface velocity seems to have reached its final value at $X = 3$ whereas no significant change in the film thickness occurs after $X > 1$. It is clearly seen from figure 4 that the X component of the surface velocity, $U_s(X)$, needs a longer time for establishment than the film thickness. While at $X = 2$, $h(X)$ was $1{\cdot}009 \times h_\infty$, $U_s(X)$ was

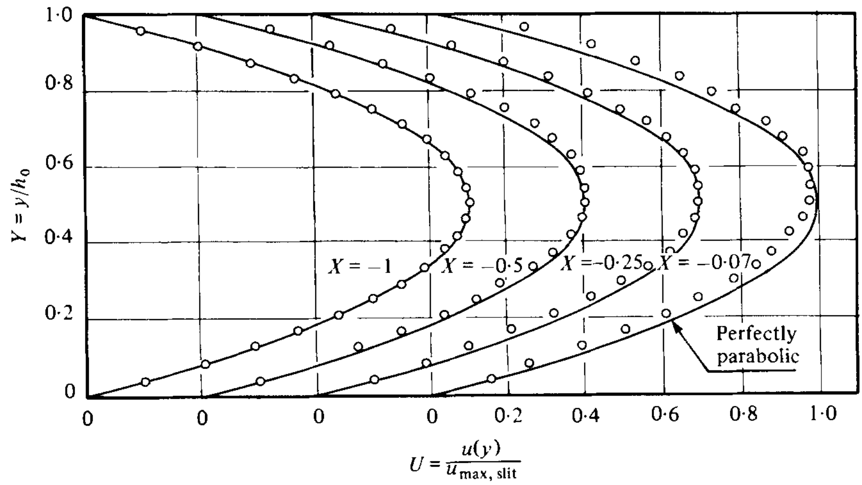

FIGURE 2. Velocity profiles near the exit of the slit; the slit exit is at $X = 0$. Data for different measuring positions are shifted horizontally by equal amounts $\Delta U = 0{\cdot}3$ for clarity. $\beta = 30°$, $h_0 = 18$ mm, $Re = Q\rho/\mu = 3{\cdot}4 \times 10^{-3}$, $u_{max} = 6{\cdot}85$ mm s^{-1}.

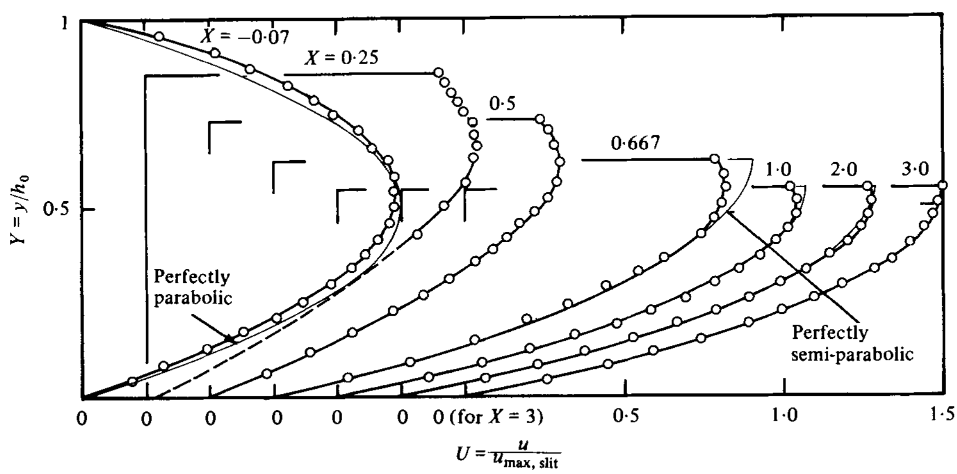

FIGURE 3. Velocity rearrangement after emerging from the slit; the slit exit is at $X = 0$. Data for different measuring positions are shifted horizontally by equal amounts $\Delta U = 0{\cdot}2$ for clarity. $\beta = 30°$, $h_0 = 18{\cdot}0$ mm.

only $0{\cdot}978 \times U_{s,\infty}$; at $X = 3, U_s(X)$ was $0{\cdot}990 \times U_{s,\infty}$ and at $X = 4$, $0{\cdot}996 \times U_{s,\infty}$. Such a difference was also found for other angles of inclination. The hydrodynamic entrance length $X_{1\%} = x/h_\infty$, defined with the x where $\Delta H = (h - h_\infty)/h_\infty = 0{\cdot}01$ is found to be twice the length $\bar{X}_{1\%} = \bar{x}/h_\infty$, defined with the x value $\bar{x}$ where

$$U_s = (u_s - u_{s,\infty})/u_{s,\infty} = 0{\cdot}01.$$

Wilkes & Nedderman (1962) had experimentally shown for Re about 1 that the relative change of the film thickness, ΔH, depends exponentially on the flow length. This is also true for $0{\cdot}0014 \leqslant Re \leqslant 0{\cdot}108$; figures 5 and 6 reproduce this result for two

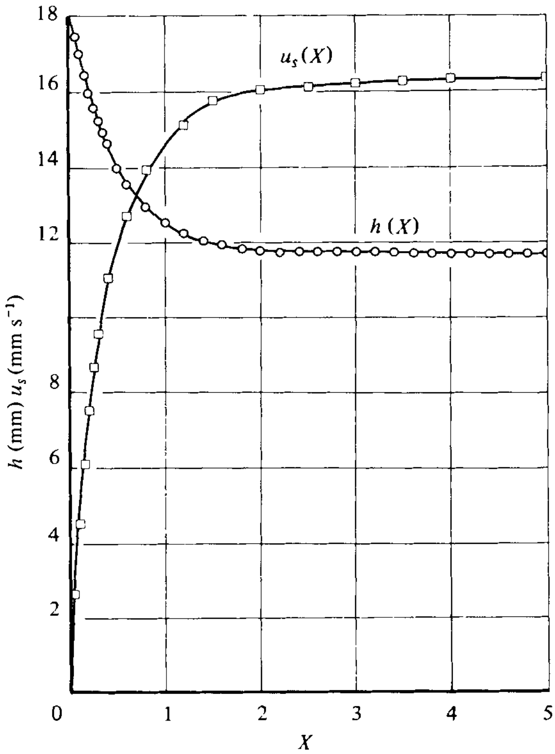

FIGURE 4. Change of the film thickness h and the surface velocity component u_s as a function of the flow distance $X = x/h_0$ on the plate. $Re = 6{\cdot}28 \times 10^{-3}$, $\beta = 30^\circ$, $h_0 = 18{\cdot}0$ mm, $h_\infty = 11{\cdot}64$ mm, $u_{s,\infty} = 16{\cdot}35$ mm s^{-1}.

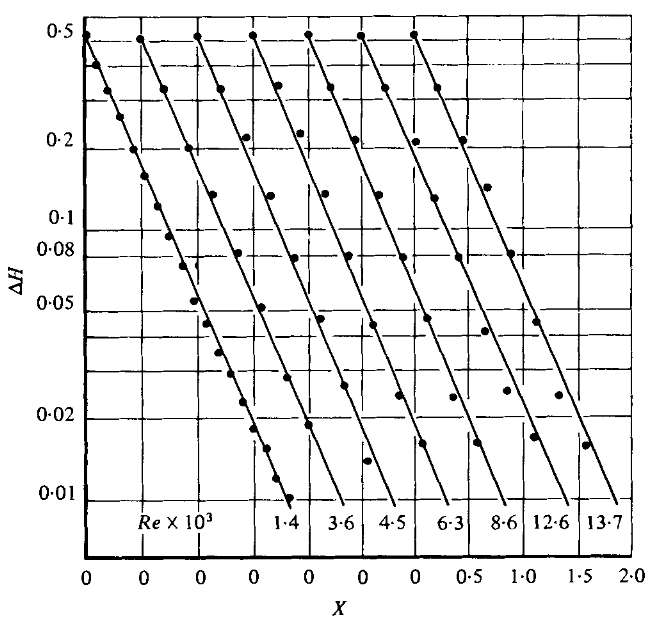

FIGURE 5. Relative change ΔH of the film thickness as a function of the flow distance X for an angle of inclination $\beta = 20^\circ$ and a slit height $h_0 = 15{\cdot}0$ mm. Data for different values of Reynolds number are shifted horizontally by equal amounts $\Delta X = 0{\cdot}5$ for clarity.

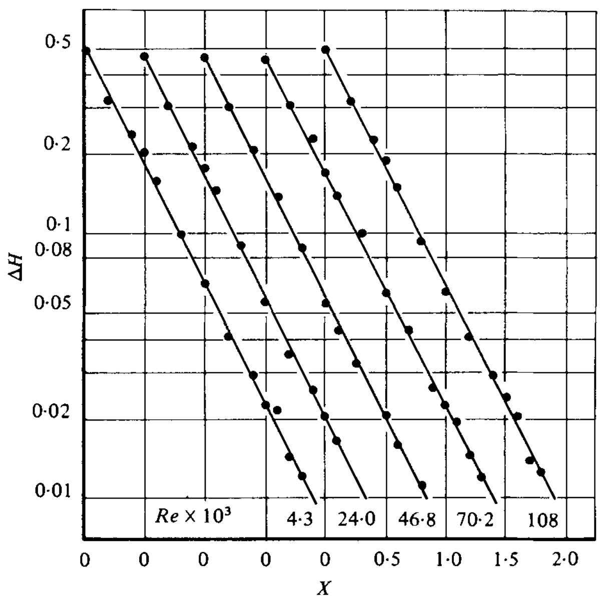

FIGURE 6. Relative change ΔH of the film thickness as a function of the flow distance X for an angle of inclination $\beta = 30°$ and a slit height $h_0 = 18{\cdot}0$ mm. Data for different values of Reynolds number are shifted horizontally by equal amounts $\Delta X = 0{\cdot}5$ for clarity.

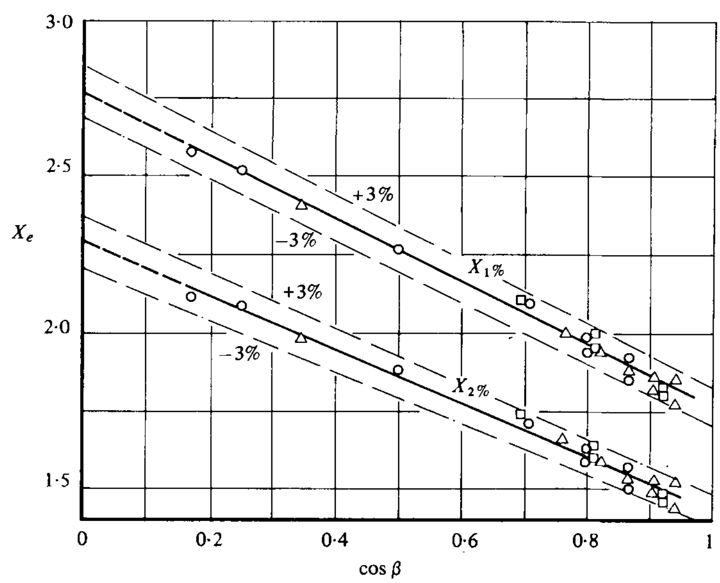

FIGURE 7. Dimensionless 1 %- and 2 %-hydrodynamic entrance lengths X_e as a function of the angle of inclination β. Measurements could be realized for $20° \leqslant \beta \leqslant 80°$. Slit height h_0: □, 10 mm; △, 15 mm; ○, 18 mm.

different angles of inclination β. It turns out that the hydrodynamic entrance length is independent of the Reynolds number – as expected for creeping flows – but is dependent on the inclination. With figure 7 we have a summary of the comprehensive experimental data for the hydrodynamic entrance length, calculated from film-

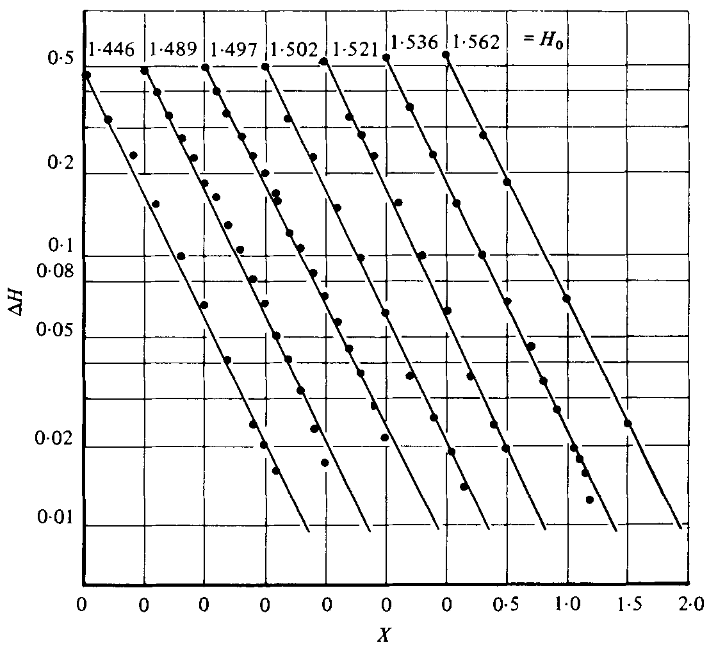

FIGURE 8. Relative change ΔH of the film thickness as a function of the flow distance X for an angle of inclination $\beta = 30°$ and a slit height h_0 18·05 mm. Data for different initial film-thickness ratios H_0 are shifted horizontally by equal amounts $\Delta X = 0{\cdot}5$ for clarity. H_0 is less, than $4^{\frac{1}{3}} = 1{\cdot}587$ due to a weak pressure gradient in the slit.

thickness measurements. Within the experimental error of $\pm 3\%$, a single empirical correlation fits the data very well:

$$X_{1\%} = 1{\cdot}77 + \cos\beta, \tag{10}$$

$$X_{2\%} = 1{\cdot}43 + 0{\cdot}86\cos\beta. \tag{11}$$

The $\cos\beta$ dependence of $X_{1\%}$ and $X_{2\%}$ is obvious from a first approximation of the x-momentum equation which yields

$$\frac{\partial p}{\partial x} \approx \rho g \cos\beta \frac{dh}{dx}. \tag{12}$$

In a detailed analysis based on the measurements done by Stücheli (1976), it is shown that the surface tension is negligible compared with $\rho g \cos\beta\, dh/dx$ but the viscous terms $\mu\, \partial^2 u_s/\partial x^2$ and $\mu\, \partial^2 u/\partial x^2$ can be of the same magnitude. The approximation of the curvature of the surface by d^2h/dx^2 differs from the true expression

$$(d^2h/dx^2)/[1+(dh/dx)^2]^{\frac{3}{2}}$$

by a factor 2 at $X = 0$ and is already negligible at $X = 0{\cdot}5$.

A weak pressure gradient within the slit giving rise to a higher film thickness which is obvious at $H_0 < 4^{\frac{1}{3}} = 1{\cdot}587$ does not influence the dimensionless hydrodynamic entrance length $X_{1\%}$ or $X_{2\%}$ as can be seen from figure 8.

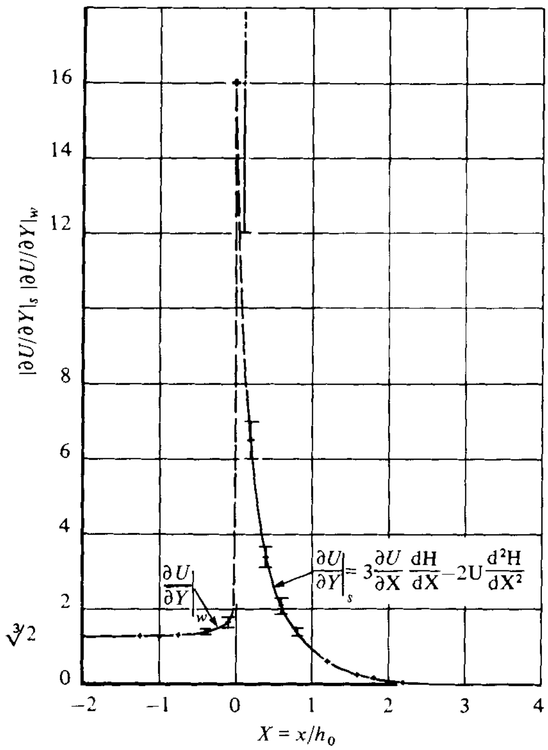

FIGURE 9. Change of the velocity gradient $\partial U/\partial Y$ at the upper slit wall (there is a shear stress) and at the free film surface where the shear stress has to be zero. $Re = 6{\cdot}28 \times 10^{-3}$, $\beta = 30°$, $h_0 = 18{\cdot}0$ mm, $h_\infty = 11{\cdot}64$ mm.

4.3. *Rise and fall of the velocity gradient $\partial U/\partial Y$*

Because of the very precise traversing system for the LDV optics, measurements were carried out close to the upper slit wall so that it was able to calculate the change of the velocity gradient along the flow direction by assuming $\partial U/\partial Y|_w \doteq \Delta U/\Delta Y$ for $\Delta Y = 0{\cdot}04y/h_0$. The fading away of $\partial U/\partial Y|_s$ was obtained with equation (6) from the results already shown in figure 4. Of course, $\partial U/\partial Y$ in figure 9 is not proportional to the shear stress except for when the streamlines become straight lines again. However, we may note the pronounced peak of $\partial U/\partial Y$ at the singular point $X = 0$.

5. Conclusion

There is a transition region twice as long for the surface velocity than for the film thickness for a creeping liquid film issuing from a slit. The hydrodynamic entrance length required for the film thickness to attain the final value h_∞ within 1 % is 1·77 to 2·77 times h_∞, depending on the inclination of the flow plane.

It is worth mentioning that the empirical equations presented here are not generally valid. For small-scale free surface flows, i.e. viscocapillary flows, the ratio of slit width to final film thickness, H, has not to be of the order of one. The interested reader may study the synthesis of Scriven and his co-workers, see Higgins *et al.* (1977).

Acknowledgement is made to the Swiss National Science Foundation which supported the work.

REFERENCES

CERRO, R. L. & WHITAKER, S. 1971 *Chem. Engng Sci.* **26**, 785.

GOREN, S. L. 1966 *J. Fluid Mech.* **25**, 87.

HIGGINS, B. G., SILLIMANN, W. J., BROWN, R. A. & SCRIVEN, L. E. 1977 *Ind. & Engng Chem. Fundam.* **16**, 393.

ITEN, P. D. & MASTNER, J. 1974 *Flow, Its Measurement and Control in Science and Industry*, vol. I (ed. R. Wendt), part 2, p. 1007. Pittsburgh.

LEGRAND, D. G. & GAINES, G. L. 1969 *J. Colloid & Interface Sci.* **31**, 162.

RUSCHAK, K. J. & SCRIVEN, L. E. 1977 *J. Fluid Mech.* **81**, 305.

SCHOWALTER, W. R. & ALLEN, R. C. 1975 *Trans. Soc. Rheol.* **19**, 129.

STÜCHELI, A. 1976 *Dissertation ETH Zürich*, no. 5785.

STÜCHELI, A. 1978 *Wärme & Stoffübertragung* **11**, 91.

STÜCHELI, A. & ÖZISIK, M. N. 1976 *Chem. Engng Sci.* **31**, 369.

WHITAKER, S. & CERRO, R. L. 1974 *Chem. Engng Sci.* **29**, 963.

WILKES, J. O. & NEDDERMAN, R. M. 1962 *Chem. Engng Sci.* **17**, 177.